??? manuscript No.
(will be inserted by the editor)

Numerical modeling of CO_2 fracturing by phase field approach

Mostafa Mollaali · Vahid Ziaei Rad · Yongxing Shen

Received: date / Accepted: date

Abstract One of the methods for enhancement of oil and gas extraction is hydraulic fracturing during which a fluid with a higher pressure than in-situ stress of the area of interest is injected to a point of well isolated by packers. we will introduce a model to simulating CO_2 fracturing by phase field to overcome the disadvantages of water based fluid in hydraulic fracturing in shale gas. The compressibility of CO_2 is significantly larger than that of either water based fracturing fluid then we can not apply the governing equation for slightly compressible fluid flow for CO_2 fracturing. We will use phase field approach to modeling fracture. The phase field approach to model fracture systems introduces a continuous field variable which differentiates between the fully broken and intact material phases. In the most classical hydraulic fracturing models, modeling the fractured system is crucial due to the need pre-knowledge for initiation of fracture, fracture path, branching and singularities at fracture tips. Recently, these difficulties are overcome by phase field approach.

Keywords CO_2 fracturing · CO_2 fluid flow · phase field

Mostafa Mollaali · Yongxing Shen
State Key Laboratory of Metal Matrix Composites
University of Michigan-Shanghai Jiao Tong University Joint Institute
Shanghai Jiao Tong University
Shanghai, China
Tel.: +86-21-34207218
E-mail: yongxing.shen@sjtu.edu.cn

Vahid Ziaei Rad
Department of .....
University ....
...., Iran

1 Introduction

Hydraulic fracturing. Hydraulic fracturing is a process where fracture propagation is driven by tensile loading by injected high-pressure fluid. It is widely applied in enhancing oil and gas production from underground reservoirs. Other important applications of this technique include extracting geothermal energy and determining *in situ* stress.

Modeling of hydraulic fracturing has attracted growing attention from researchers and engineers since 1950s. The pioneering papers by Khristianovic and Zheltov [19] and by Geertsma and de Klerk (KGD) [15] marked the beginning of hydraulic fracturing modeling. Despite extensive research on this subject, the numerical modeling of fluid-driven fractures remains a challenging problem. It includes at least three distinct ingredients: solid deformation, fluid flow in fracture, and fracture propagation. The solid deformation is usually simulated using linear elasticity theory, and fracture propagation is normally modeled with Griffith's theory. Review of the overall simulation technique can be found in [14, 1].

Shale gas. Shale gas is the natural gas that is trapped within the shale, or mudstone reservoir, is the most common sedimentary rock. Shale gas has become increasingly interested energy source in all of the world. In 2010, 20% of of U.S. natural gas production was provided by shale gas. While by prediction of the U.S. government's Energy Information Administration, 46% of the United States' natural gas supply will come from shale gas by 2035 [22]. China is estimated to have the largest recoverable shale gas reservoirs [2].

Shale is a fine-grained, sedimentary rock composed of clay minerals and silt-sized particles, and consisting of other minerals such as quartz, calcite, and pyrite. However, shale has low permeability [16]. Since the low permeability of shale greatly inhibits the flow of gas from reservoir rocks to production wells, the economic viability of developing shale gas depends on effective stimulation of reservoirs. Presently, horizontal wells employing a multistage hydraulic fracturing technique is drawing attention around of the world [23].

Recently, the water base-fluid are most important fluids that regularly use in the commercial shale gas due to ready availability, low cost. But there are some disadvantages to use water based fluid, namely: water shortage, contamination of underground water, and low fracturing performance. Also, hydraulic fracturing can not avoid the clay swelling problem in shale [23]. Due to these problems, researchers encourage to using non-aqueous and non fluid fracturing such as explosive based method.

Carbon dioxide is one of non-aqueous fracturing fluid that is considered to use in hydraulic fracturing. Carbon dioxide as a hydraulic fracturing fluid has been successfully applied in fracturing unconventional gas reservoirs decades ago [21]. Since the critical temperature of carbon dioxide is $31.1C$, once the pressure exceeds its critical pressure of 7.38 MPa it will be change to supercritical state [28]. It can be injected down-hole either be in liquid or supercritical state. The principal benefits of carbon dioxide as a fracturing fluid includes

reducing consumption of water and water contamination. Also, carbon dioxide is highly miscible with oil and gas. In particular, the loss of CO2 to the atmosphere should be avoided because of eventual impact on global warming. CO2 fracturing keeps clays (smectite and illite) stabilized and prevents metal leaching and chemical interactions.

Phase field. Phase field modeling of fracture has gained popularity since the beginning of this century. What makes the phase field an attractive approach can be attributed to its convenience on simulating complex fracture processes, including crack initiation, propagation, branching and merging. Compared to discrete fracture descriptions, the phase field approaches avoid tracking the complicated crack geometry; instead, the crack evolution is a natural outcome of the numerical solution to a set of coupled partial differential equations. Thus, it significantly decreases the implementation difficulty, especially when dealing with 3D problems.

Phase field models have been developed in the physics, the mathematics and mechanics communities; however, the theoretical and technical backgrounds for developing the constitutive models and formulations are completely different. In the physics communities, phase field models originated from the phase field evolution equations presented by Landau and Ginzburg [20]. Here we list several representative models: the Aranson-Kalatsky-Vinokur model [5], the Karma-Kessler-Levine model [18], and the Henry-Levine model [17]. For more details and comparisons, readers are referred to [3].

In contrast, the phase field models developed in the mathematics and mechanics communities are based on Griffith's theory. The origin of this kind of models is due to the variational formulation of brittle fracture by Francfort and Marigo [13], and the regularized implementation by Bourdin et al. [9].

Mostafa: Complete the intoduction To Do

Mostafa: what's the novility and objective of this work? To Do

CO_2 fluid flow.

Motivation.

The structure of paper.

2 Mathematical model

Let $\Omega \subset \mathbb{R}^n$, $n = 2, 3$, be a bounded domain with a Lipschitz continuous boundary. Linear elastostatics on Ω can be formulated as minimizing the fol-

lowing potential energy

$$\Pi[\boldsymbol{u}] := \int_{\Omega} \psi_0[\boldsymbol{\varepsilon}(\boldsymbol{u})]\, d\Omega - \int_{\Gamma_N} \boldsymbol{t}_N \cdot \boldsymbol{u}\, d\Gamma - \int_{\Omega} \boldsymbol{b} \cdot \boldsymbol{u}\, d\Omega, \tag{1}$$

where $\boldsymbol{u} \in H^1(\Omega; \mathbb{R}^n)$ is the displacement field, Γ_D and Γ_N satisfy that $\Gamma_D \cup \Gamma_N = \partial\Omega$ and $\Gamma_D \cap \Gamma_N = \emptyset$, and $\boldsymbol{u}_D : \Gamma_D \to \mathbb{R}^n$ and $\boldsymbol{t}_N : \Gamma_N \to \mathbb{R}^n$ are prescribed displacement and traction boundary conditions, respectively. Vector fields $\boldsymbol{b} : \Omega \to \mathbb{R}^n$ and $\boldsymbol{t}_N$ are body force per unit volume and traction force, respectively. Operator $\boldsymbol{\varepsilon}$ gives the symmetric part of the gradient of a vector field:

$$\boldsymbol{\varepsilon}(\boldsymbol{u}) := \frac{1}{2}\left(\nabla \boldsymbol{u} + \nabla \boldsymbol{u}^T\right).$$

When $\boldsymbol{\varepsilon}$ is applied to the displacement field $\boldsymbol{u}$, the strain field is obtained, which will also be denoted as $\boldsymbol{\varepsilon}$.

The strain energy density for a linear isotropic material is given by

$$\psi_0(\boldsymbol{\varepsilon}) := \frac{\lambda}{2}(\operatorname{tr} \boldsymbol{\varepsilon})^2 + \mu \boldsymbol{\varepsilon} : \boldsymbol{\varepsilon}, \tag{2}$$

with λ and μ Lamé constants such that $\mu > 0$ and $\lambda + 2\mu > 0$.

Phase field. The phase field approach to model brittle fracture consists in minimizing the system's total energy functional, which is the sum of the elastic potential energy and the energy due to the presence of cracks. We consider the same domain as that in Section **??**. In addition, let $\Gamma_P \subset \Omega$ be the region of pre-exisiting cracks.

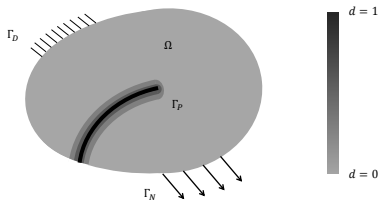

Fig. 1: Sharp and diffusive crack topology. (a) A domain Ω with a sharp crack surface Γ. (b) The regularized crack surface is represented by the phase field d, $0 \le d \le 1$. The region with $d = 0$ indicates where the material is at the pristine state while $d = 1$ indicates the fully broken state. A pre-existing crack is represented by Γ_P, over which we impose $d = 1$. The width of the region with $d > 0$ is on the order of ℓ in the AT1 model.

Herein, we first introduce the regularized crack functional to approximate the fracture energy, which reads:

$$\Gamma_\ell(d) = g_c \int_{\Omega} \gamma(d, \nabla d)\, d\Omega \tag{3}$$

where d represents the phase field, characterizing the material at its pristine state with $d = 0$ and that at the fully broken state with $d = 1$, as depicted in Figure **??**. Scalar $g_c > 0$ represents the critical Griffith-type fracture energy release rate, or the material fracture toughness. Function $\gamma(d, \nabla d)$ is the crack surface density function, which is defined as:

$$\gamma(d, \nabla d) = \frac{1}{4c_w}\left(\frac{w(d)}{\ell} + \ell|\nabla d|^2\right), \tag{4}$$

where $\ell > 0$ is the regularized length parameter, which controls the width of the smooth crack approximation [10]. Constant $c_w = \int_0^1 \sqrt{w(d)}$ is a normalization constant such that when $\ell \to 0$, the regularized crack surface approximated by the phase field converges to the sharp crack surface. Classical examples of $w(d)$ are $w(d) = d^2$ and $c_w = 1/2$ for the AT2 model, and $w(d) = d$ and $c_w = 2/3$ in the AT1 model.

An alternative to (4) is the expression in the fourth order phase field proposed by Borden *et al.* [8]:

$$\gamma(d, \nabla d, \Delta d) = \frac{1}{4\ell}\left[d^2 + 2\ell^2|\nabla d|^2 + \ell^4(\Delta d)^2\right].$$

In the formulations below, we will confine ourselves to the form (4).

Generalized from the elastostatic case, the phase field formulation for brittle fracture is essentially based on minimization of the following functional:

$$\Pi_\ell[\boldsymbol{u}, d] := \int_\Omega \psi[\boldsymbol{\varepsilon}(\boldsymbol{u}), d]\, d\Omega - \int_{\Gamma_N} \boldsymbol{t}_N \cdot \boldsymbol{u}\, d\Gamma - \int_\Omega \boldsymbol{b}\cdot\boldsymbol{u}\, d\Omega + g_c \int_\Omega \gamma(d, \nabla d)\, d\Omega. \tag{5}$$

We keep the strain energy density $\psi[\boldsymbol{\varepsilon}(\boldsymbol{u}), d]$ in the general form:

$$\psi(\boldsymbol{\varepsilon}, d) = g(d)\psi_+(\boldsymbol{\varepsilon}) + \psi_-(\boldsymbol{\varepsilon}),$$

where $g(d)$ is the degradation function, which models the partial loss of stiffness due to the presence of cracks. The minimum requirement on $g(d)$ is $g(0) = 1$, $g(1) = 0$, and $g'(d) < 0$ for all $d \in (0, 1)$. A usual choice is $g(d) = (1 - d)^2 + k$, with k a small number, which can be taken as, e.g., 1×10^{-10}. Borden [7], Karma *et al.* [18], and Sargado *et al.* [26] proposed cubic, quartic, and exponential degradation functions, respectively.

Functions $\psi_\pm(\boldsymbol{\varepsilon})$ should satisfy

$$\psi_+(\boldsymbol{\varepsilon}) + \psi_-(\boldsymbol{\varepsilon}) = \psi_0(\boldsymbol{\varepsilon}),$$

where ψ_0 was defined in (2).

The Cauchy stress tensor taking into account the phase field d becomes

$$\boldsymbol{\sigma} = \frac{\partial\psi}{\partial\boldsymbol{\varepsilon}} = g(d)\boldsymbol{\sigma}_+(\boldsymbol{\varepsilon}) + \boldsymbol{\sigma}_-(\boldsymbol{\varepsilon})$$

with $\boldsymbol{\sigma}_\pm(\boldsymbol{\varepsilon}) := \partial\psi_\pm/\partial\boldsymbol{\varepsilon}$.

Specific phase field models. Here we list three representative phase field models that differ in their choice of ψ_+, and thus different expressions of $\boldsymbol{\sigma}(\boldsymbol{\varepsilon}, d)$ and $\mathbb{C}(\boldsymbol{\varepsilon}, d)$.

Model A. The "isotropic" model proposed by [9]. In this model,

$$\psi_+(\boldsymbol{\varepsilon}) = \psi_0(\boldsymbol{\varepsilon}), \quad \psi_-(\boldsymbol{\varepsilon}) = 0.$$

Hence

$$\boldsymbol{\sigma}(\boldsymbol{\varepsilon}, d) = g(d)\frac{\partial \psi_0(\boldsymbol{\varepsilon})}{\partial \boldsymbol{\varepsilon}} = g(d)\left[\lambda(\operatorname{tr}\boldsymbol{\varepsilon})\mathbf{1} + 2\mu\boldsymbol{\varepsilon}\right],$$

and

$$\mathbb{C}(\boldsymbol{\varepsilon}, d) = g(d)\left[\lambda \mathbf{1}\otimes\mathbf{1} + 2\mu\mathbb{I}\right],$$

where $\otimes$ is the dyadic operator.

In indicial notations,

$$\begin{aligned}\sigma_{ij}(\boldsymbol{\varepsilon}, d) &= g(d)\left[\lambda\varepsilon_{kk}\delta_{ij} + 2\mu\varepsilon_{ij}\right],\\ \mathbb{C}_{ijkl}(\boldsymbol{\varepsilon}, d) &= g(d)\left[\lambda\delta_{ij}\delta_{kl} + \mu(\delta_{ik}\delta_{jl} + \delta_{il}\delta_{jk})\right].\end{aligned}$$

It can be seen that $\mathbb{C}$ is modified by just multiplying $g(d)$ to (**??**). Hence, if an existing code for the standard finite element is available, only a simple modification is needed to render a phase field element code, i.e., by multiplying the factor $g(d)$ to the stress and elasticity tensors. Moreover, the half problems for solving $\boldsymbol{u}$ and d in alternate minimization are both linear, see Section **??**.

It is worth mentioning that Ambati *et al.* [3] introduced a hybrid formulation that contains features of Models A and B, aiming at reducing the computational costs compared with the other nonlinear models. In particular, the constitutive model therein is the same as Model A.

Model B. This is due to Amor *et al.* [4]. They have

$$\psi_+(\boldsymbol{\varepsilon}) = \frac{K}{2}\langle \operatorname{tr}\boldsymbol{\varepsilon}\rangle_+^2 + \mu\|\operatorname{dev}\boldsymbol{\varepsilon}\|^2, \quad \psi_-(\boldsymbol{\varepsilon}) = \frac{K}{2}\langle \operatorname{tr}\boldsymbol{\varepsilon}\rangle_-^2,$$

where $\langle a\rangle_\pm := (a \pm |a|)/2$[1] and the bulk modulus $K = \lambda + 2\mu/3$. Thus,

$$\boldsymbol{\sigma}(\boldsymbol{\varepsilon}, d) = g(d)\left(K\langle \operatorname{tr}\boldsymbol{\varepsilon}\rangle_+\mathbf{1} + 2\mu\operatorname{dev}\boldsymbol{\varepsilon}\right) + K\langle \operatorname{tr}\boldsymbol{\varepsilon}\rangle_-\mathbf{1},$$

and

$$\mathbb{C}(\boldsymbol{\varepsilon}, d) = g(d)\left[KH(\operatorname{tr}\boldsymbol{\varepsilon})\mathbf{1}\otimes\mathbf{1} + 2\mu\left(\mathbb{I} - \frac{1}{3}\mathbf{1}\otimes\mathbf{1}\right)\right] + KH(-\operatorname{tr}\boldsymbol{\varepsilon})\mathbf{1}\otimes\mathbf{1},$$

where H is the Heaviside function, such that $H(a) = 1$ if $a > 0$, $H(a) = 0$ if $a < 0$, and $H(a) = 1/2$ for $a = 0$ for symmetry.

[1] Note that we are using a different convention than that in [25], where $\langle a\rangle_\pm$ was defined as $(|a| \pm a)/2$.

Fracking by phase field in porous media. For modeling hydraulic fracturing we need to account to fracture fluid pressure in porous media. The total functional energy of phase field that proposed in (5) to contribute the work that is done by fracturing fluid.

With assuming the fluid pressure continuity $p = p_f$ on Γ and $p = p_R$ on $\Omega\backslash\Gamma$ and using phase field calculus, we can extend the work done by the fracturing fluid pressure on the fracture surfaces, p_f, to entire the computational domain

$$\int_{\Gamma} p\,[|\boldsymbol{u}|]\cdot n_{\Gamma} \approx \int_{\Omega} p\boldsymbol{u}\cdot\nabla d\; d\Omega \tag{6}$$

The work of the pressure forces is added to (5) to provide an updated total energy formulation applicable to hydraulic fracturing

$$\Pi_{\ell}[\boldsymbol{u},d] := \int_{\Omega}\psi[\boldsymbol{\varepsilon}(\boldsymbol{u}),d]\; d\Omega - \int_{\Gamma_N}\boldsymbol{t}_N\cdot\boldsymbol{u}\; d\Gamma - \int_{\Omega}\boldsymbol{b}\cdot\boldsymbol{u}\; d\Omega + g_c\int_{\Omega}\gamma(d,\nabla d)\; d\Omega + \int_{\Omega} p\boldsymbol{u}\cdot\nabla d\; d\Omega. \tag{7}$$

Also, the poroelastic strain energy density for contributing pore pressure through effective stress denotes as follow

Mostafa: check this formulation is used in the code or Bourdin 2012

- Bourdin 2012, the formulation is just for a pressurized fracture
- Wheeler 2014, the formulation is just for a pressurized fracture in porous media , then the term of α exists in formulation.
- Bourdin 2016, the formulation is for a hydraulic fracturing in porous media, then the term of α exists in formulation.

You need be clear about formulation in code and paper

To Do

$$\psi[\boldsymbol{\varepsilon}(\boldsymbol{u}),d] = \frac{1}{2}\mathbb{C}(d\boldsymbol{\varepsilon}(\boldsymbol{u}) - \frac{\alpha}{3\kappa}\mathbb{I}p) : (d\boldsymbol{\varepsilon}(\boldsymbol{u}) - \frac{\alpha}{3\kappa}\mathbb{I}p) \tag{8}$$

where $\alpha \in [0,1]$ and κ are Biot coefficient and drained bulk modulus of the material, respectively.

2.1 Compressible (CO_2) fluid flow

The generalized equation of fluid flow, governed by the laws of conservation of mass, can be written as follows

$$\frac{\partial(\phi\rho)}{\partial t} + \nabla\cdot\left(-\rho\frac{k}{\mu}\nabla p\right) = 0 \tag{9}$$

To Do

Mostafa: add the flow rate in (9), and change the terms related to it

where ρ is fluid density that it's a function of pressure under isothermal condition; μ is dynamic fluid viscosity; k and ϕ are the permeability of the rock and porosity, respectively; With expanding the LHS and RHS (9), we get

$$\frac{\partial(\phi\rho)}{\partial t} = \rho\frac{\partial\phi}{\partial t} + \phi\frac{\partial\rho}{\partial t} = \phi\left[\frac{\partial\rho}{\partial p}\frac{\partial p}{\partial t}\right] + \rho\frac{\partial\varepsilon_v}{\partial t} \tag{10}$$

$$\nabla\cdot\left(-\rho\frac{k}{\mu_g}\nabla p\right) = \nabla\cdot\left(-\rho\frac{k}{\mu_g}\right)\nabla p - \rho\frac{k}{\mu_g}\nabla^2 p = -\frac{k}{\mu_g}\left[\frac{d\rho}{dp}(\nabla p)^2 + \rho\nabla^2 p\right] \tag{11}$$

It is worth to mention, we suppose the change of pore volume is equal to the change of strain volume.

The gas density varies significantly with pressure under isothermal condition, that will be described by the equation of state. Span and Wagner [27] have proposed one of applicable equation of state for carbon dioxide that is a fundamental equation expressed in form of the Helmholtz energy. They introduced the residual part of the Helmholtz energy as follow

$$\varphi^r(\delta,\tau) = \sum_{i=1}^{7} n_i\delta^{d_i}\tau^{t_i} + \sum_{i=8}^{34} n_i\delta^{d_i}\tau^{t_i}e^{-\delta^{c_i}} + \sum_{i=35}^{39} n_i\delta^{d_i}\tau^{t_i}e^{-\alpha_i(\delta-\varepsilon_i)^2-\beta_i(\tau-\gamma_i)^2} + \sum_{i=40}^{42} n_i\Delta^{b_i}\delta e^{C_i(\delta-1)^2-D_i(\tau-1)^2} \tag{12}$$

where

$$\Delta = \left\{(1-\tau) + A_i\left[(\delta-1)^2\right]\frac{1}{2\beta_i}\right\}^2 + B_i\left[(\delta-1)^2\right]^{a_i}$$

where $\delta = \rho/\rho_c$ and $\tau = T/T_c$ are reduced density and temperature, respectively. Also, ρ_c and T_c are the critical density and temperature, respectively. Other Coefficients and exponents of (12) are constant and denote in table 1.

To Do

Mostfa: I think we do not need put this table here, just cite the referenc.

The CO2 density and pressure are related to each other with

$$p = (1+\delta\varphi_\delta^r)\,\rho RT \tag{13}$$

To Do

Mostafa: we need add a figure to show the relation of pressure, density and tempreture (Eqution of state)

Table 1: Coefficient and exponents of (12) [27]

i	n_i	d_i	t_i					
1	$0.388\,568\,232\,031\,61\times10^{0}$	1	0.00					
2	$0.293\,854\,759\,427\,40\times10^{1}$	1	0.75					
3	$-0.558\,671\,885\,349\,34\times10^{1}$	1	1.00					
4	$-0.767\,531\,995\,924\,77\times10^{0}$	1	2.00					
5	$0.317\,290\,055\,804\,16\times10^{0}$	2	0.75					
6	$0.548\,033\,158\,977\,67\times10^{0}$	2	2.00					
7	$0.122\,794\,112\,203\,35\times10^{0}$	3	0.75					
i	n_i	d_i	t_i	c_i				
8	$0.216\,589\,615\,432\,20\times10^{1}$	1	1.50	1				
9	$0.158\,417\,351\,097\,24\times10^{1}$	2	1.50	1				
10	$-0.231\,327\,054\,055\,03\times10^{0}$	4	2.50	1				
11	$0.581\,169\,164\,314\,36\times10^{-1}$	5	0.00	1				
12	$-0.553\,691\,372\,053\,82\times10^{0}$	5	1.50	1				
13	$0.489\,466\,159\,094\,22\times10^{0}$	5	2.00	1				
14	$-0.242\,757\,398\,435\,01\times10^{-1}$	6	0.00	1				
15	$0.624\,947\,905\,016\,78\times10^{-1}$	6	1.00	1				
16	$-0.121\,758\,602\,252\,46\times10^{0}$	6	2.00	1				
17	$-0.370\,556\,852\,700\,86\times10^{0}$	1	3.00	2				
18	$-0.167\,758\,797\,004\,26\times10^{-1}$	1	6.00	2				
19	$-0.119\,607\,366\,379\,87\times10^{0}$	4	3.00	2				
20	$-0.456\,193\,625\,087\,78\times10^{-1}$	4	6.00	2				
21	$0.356\,127\,892\,703\,46\times10^{-1}$	4	8.00	2				
22	$-0.744\,277\,271\,320\,52\times10^{-2}$	7	6.00	2				
23	$-0.173\,957\,049\,024\,32\times10^{-2}$	8	0.00	2				
24	$-0.218\,101\,212\,895\,27\times10^{-1}$	2	7.00	3				
25	$0.243\,321\,665\,592\,36\times10^{-1}$	3	12.00	3				
26	$-0.374\,401\,334\,234\,63\times10^{-1}$	3	16.00	3				
27	$0.143\,387\,157\,568\,78\times10^{0}$	5	22.00	4				
28	$-0.134\,919\,690\,832\,86\times10^{0}$	5	24.00	4				
29	$-0.231\,512\,250\,534\,80\times10^{-1}$	6	16.00	4				
30	$0.123\,631\,254\,929\,01\times10^{-1}$	7	24.00	4				
31	$0.210\,583\,219\,729\,40\times10^{-2}$	8	8.00	4				
32	$-0.339\,585\,190\,263\,68\times10^{-3}$	10	2.00	4				
33	$0.559\,936\,517\,715\,92\times10^{-2}$	4	28.00	5				
34	$-0.303\,351\,180\,556\,46\times10^{-3}$	8	14.00	6				
i	n_i	d_i	t_i	α_i	β_i	γ_i	ϵ_i	
35	$-0.213\,654\,886\,883\,20\times10^{3}$	2	1.00	25	325	1.16	1.00	
36	$0.266\,415\,691\,492\,72\times10^{5}$	2	0.00	25	300	1.19	1.00	
37	$-0.240\,272\,122\,045\,57\times10^{5}$	2	1.00	25	300	1.19	1.00	
38	$-0.283\,416\,034\,239\,99\times10^{3}$	3	3.00	15	275	1.25	1.00	
39	$0.212\,472\,844\,001\,79\times10^{3}$	3	3.00	20	275	1.22	1.00	
i	n_i	a_i	b_i	β_i	A_i	B_i	C_i	D_i
40	$-0.666\,422\,765\,407\,51\times10^{0}$	3.500	0.875	0.300	0.700	0.3	10.0	275
41	$0.726\,086\,323\,498\,97\times10^{0}$	3.500	0.925	0.300	0.700	0.3	10.0	275
42	$0.550\,686\,686\,128\,42\times10^{-1}$	3.000	0.875	0.300	0.700	1.0	12.5	275

[a] $R = 0.188\,924\,1$ kJ/(kg K); $T_c = 304.128\,2$ K; $\rho_c = 467.6$ kg/m^3.

where R is the universal gas constant; and $\delta\varphi_\delta^r$ is the derivative of the residual part of the Helmholtz free energy with respect to the reduced density. The derivative of pressure respect to density define as follow:

$$\begin{aligned}\frac{\partial p}{\partial \rho} =& RT\left(1+\delta\varphi_\delta^r\right)+\rho RT\frac{\partial\left(\delta\varphi_\delta^r\right)}{\partial\rho}=RT\left(1+\delta\varphi_\delta^r\right)+\rho RT\varphi_\delta^r\frac{\partial\delta}{\partial\rho}+\rho RT\varphi_\delta^r\frac{\partial\varphi_\delta^r}{\partial\rho}\\ =& RT\left(1+2\delta\varphi_\delta^r+\delta^2\varphi_{\delta\delta}^r\right)=N\end{aligned} \tag{14}$$

where $\delta\varphi_\delta^r$ and $\delta^2\varphi_{\delta\delta}^r$ are first and second derivatives of φ^r with respect to δ, respectively. Substituting (10), (11) and (14) in mass balance, (9), the governing equation for CO_2 flow is written as follows

To Do

Mostafa: $\delta\varphi^r_\delta$ and $\delta^2\varphi^r_{\delta\delta}$ are first and second derivatives of φ^r with respect to δ
or
φ^r_δ and $\varphi^r_{\delta\delta}$ are first and second derivatives of φ^r with respect to δ
check the reference [27]

$$\frac{\phi}{N}\frac{\partial p}{\partial t} + \rho\frac{\partial \varepsilon_v}{\partial t} - \frac{k}{\mu_g}\left[\frac{\phi}{N}\left(\nabla p\right)^2 + \rho\nabla^2 p\right] = 0, \tag{15}$$

that we neglect the quadratic term of pressure for simplicity in this paper. While, the mass conservation for incompressible fluid defined as follow [12]

$$\left(\frac{\phi}{K_f} + \frac{\alpha-\phi}{K_s}\right)\frac{\partial p}{\partial t} + \alpha\frac{\partial \varepsilon_v}{\partial t} - \frac{k}{\mu_g}\nabla^2 p = 0 \tag{16}$$

To Do

Mostafa: it seems strange, there is no α term in (15)

3 Numerical algorithm

To Do

Mostafa: how do we compute density, and N in each time step

Algorithm 1: Algorithm for modeling the $sc-CO_2$ by phase field.

Input: p_0, d_0
Output: $\boldsymbol{u}$, p, and d
Construct d-field, d_0;
Set flow and mechanical boundary conditions (σ_1, σ_2, Δp);
Set initial pore pressure(p);
Set $n = 1$;
repeat
  Set $k = 0, m = 0$, and $t = n\Delta t$;
  $p^k \leftarrow p_{n-1}$, and $d^m \leftarrow d_{n-1}$;
  repeat
    Step-P: compute p, (15);
    $p_{n-1} \leftarrow p$;
    $k + 1 \leftarrow k$
  until $\varepsilon_p = \left|\frac{p^{k+1} - p_{n-1}}{p^{k+1}}\right| < \varepsilon_{tol}$;
  repeat
    Step-U: compute $\mathbf{u}$, (3) ;
    Step-d: compute d, (3);
    $d_{n-1} \leftarrow d$;
    $m + 1 \leftarrow m$
  until $\varepsilon_d = \left\|d^{m+1} - d_{n-1}\right\|_\infty < \varepsilon_{tol}$;
  $n + 1 \leftarrow n$
until *the constraint* $t > t_{total}$ *is satisfied;*;

4 Numerical examples

We perform two different numerical cases. First we conduct a propagating fracture with increasing fluid pressure. As second case, we consider interaction of two fracture due to increasing the fluid pressure.....

```
Mostafa: we need mention the solver properties (PETScTAO) ,
we can use more detail about solvers such as Bilgen2018 [6]
```

To Do

4.1 Fracture propagation

We start with two classical benchmark problems, such as the single-edge notched tension and shear tests.....

```
Mostafa: we need add two exampls for single-edge notched
tention and shear according to Miehe [24]
```

To Do

To Do

Mostafa: The results thst we will show here are:

- The crack patterns at several stages of loading for model A and B (2 dimensions)
- The load-displacement curves for model A and B

Hint: it seems Miehe used the quadrilateral elements, we use triangular element

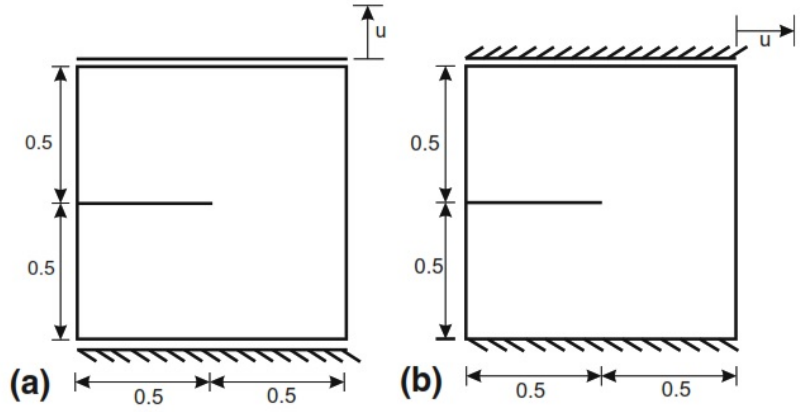

Fig. 2: The single-edge notched tension and shear

4.2 Pressurized fracture with time dependent constant pressure

We consider a 2D problem, with the following geometric data:$\Omega = (0, 4)^2$ and a initial central fracture with length $l = 0.4$ on $\Omega_c = (1.8, 2.2)\times(2-h, 2-h) \subset \Omega$. We assume zero displacements on $\partial\Omega$. Also, we set phase field value, d, one on prescribed (initial) fracture and zero on $\partial\Omega$. We use injected pressure $p = k\bar{p}$ that will be increased to drive the deformation and fracture propagation. where $\bar{p} = 0.1$ and $k = 1, 2 \cdots 15$, is time step.

The Biot coefficient α is zero. The Young modulus and Poission's ratio are chosen $E = 1$ and $\nu = 0.2$, respectively. Also, the fracture toughness is $G_c = 1$. ℓ and k are chosen h_{max} and 10^{-12}, respectively.

To Do

Mostafa: rewrite tis part, these two paragraphs are a part of a PhD theses. [11]

*Sneddon's 2D benchmark with constant pressure.*This section simulates the deformation of a static line crack in an infinite two dimensional domain. This is

the classic problem solved by Sneddon and Lowengrub (1969). The material is composed of a homogeneous isotropic. The domain is under plain strain conditions and the boundary conditions on the material is such that displacement and stresses vanish at infinity while the crack surface is acted upon by a uniform pressure p. The pre-existing line crack is non propagating and the objective is to obtain the fracture opening displacement and the fracture volume for a uniform pressure, p, acting on the crack surface. For the condition where the crack is found in the region defined by $y = 0$, $-l_0 \leq x \leq l_0$, Sneddon and Lowengrub (1969) derived the following analytical expression for the crack opening displacement in the y-direction.

$$u_y(x,0) = \frac{2(p-\sigma_0)l_0}{E'}\sqrt{1-\frac{x_0}{l_0}} \tag{17}$$

where $E' = \dfrac{E}{1-\nu^2}$. The fracture displacement profile is elliptic as evident from Equation (17). Thus, the fracture

$$V_f = \pi\frac{2(p-\sigma_0)l_0^2}{E'}$$

*Compute the fracture width and volume.*Bourdin proposed a variational formulation for fracture opening:

$$w = \boldsymbol{u}\cdot n_\Gamma \simeq \int_s \boldsymbol{u}\cdot\nabla d\, dx$$

Fracture volume is the integral of fracture width along the path of the fracture:

$$V_f = \int_\Gamma w\, ds \simeq \int_\Omega \boldsymbol{u}\cdot\nabla d\, d\Omega$$

4.3 Fracture interaction due to increasing fluid pressure

As the second example we conduct an interaction of two fractures by phase field where the fluid pressure is increased. We keep all parameters as the previous example. The initial fractures length are $l_0 = 0.4$ on on $\Omega_c = (1.8, 2.2) \times (2 - h, 2 - h) \subset \Omega$ and $\Omega_c = (2.6 - h, 2.6 - h) \times (1.8, 2.2) \subset \Omega$. Also, we set phase field value, d, one on both prescribed (initial) fracture. Figure **??** shows the the phase field contour of jointing fracture due to increasing fluid pressure.

4.4 Pressurized fracture coupled with incompressible flow

As we suppose there exist pre-existing fracture, we can not find the breakdown pressure, then we can not verify the results with experimental results of Ishida 2012, 2015!!

To Do

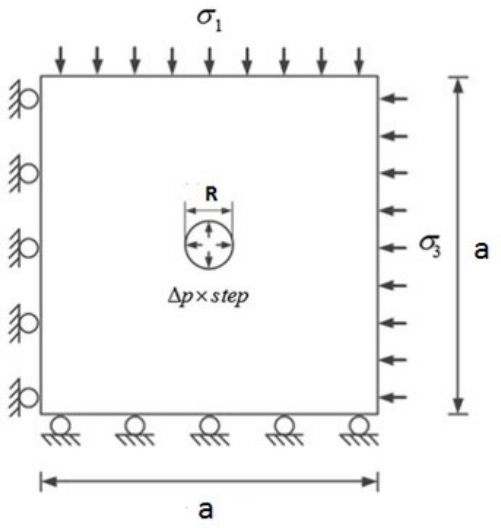

Fig. 3: 2D plane cross-section through a cubical specimen containing a central

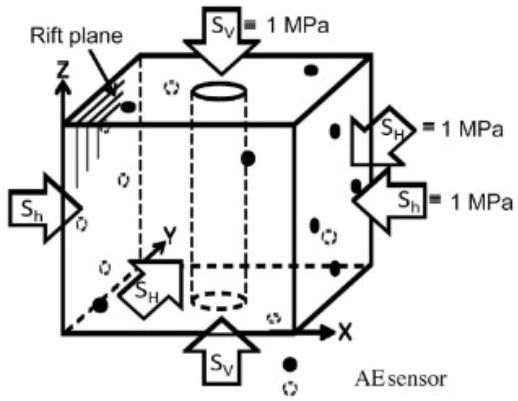

Fig. 4: 3D cubical specimen containing a central borehole

4.5 Pressurized fracture coupled with compressible flow

5 Conclusions

Acknowledgements This work is supported by the National Natural Science Foundation of China with grant #11402146. YS also acknowledges the financial support by the Young 1000 Talent Program of China.

References

1. Adachi, J., Siebrits, E., Peirce, A., Desroches, J.: Computer simulation of hydraulic fractures. International Journal of Rock Mechanics and Mining Sciences **44**(5), 739–757 (2007)
2. Administration, U.S.E.I., Kuuskraa, V.: World shale gas resources: an initial assessment of 14 regions outside the United States. US Department of Energy (2011)
3. Ambati, M., Gerasimov, T., De Lorenzis, L.: A review on phase-field models of brittle fracture and a new fast hybrid formulation. Computational Mechanics **55**(2), 383–405 (2015)
4. Amor, H., Marigo, J.J., Maurini, C.: Regularized formulation of the variational brittle fracture with unilateral contact: Numerical experiments. Journal of the Mechanics and Physics of Solids **57**, 1209–1229 (2009)
5. Aranson, I., Kalatsky, V., Vinokur, V.: Continuum field description of crack propagation. Physical Review Letters **85**(1), 118 (2000)
6. Bilgen, C., Kopaničáková, A., Krause, R., Weinberg, K.: A phase-field approach to conchoidal fracture. Meccanica **53**(6), 1203–1219 (2018). DOI 10.1007/s11012-017-0740-z. URL https://doi.org/10.1007/s11012-017-0740-z
7. Borden, M.J.: Isogeometric analysis of phase-field models for dynamic brittle and ductile fracture. Ph.D. thesis, University of Texas at Austin (2012)
8. Borden, M.J., Hughes, T.J., Landis, C.M., Verhoosel, C.V.: A higher-order phase-field model for brittle fracture: Formulation and analysis within the isogeometric analysis framework. Computer Methods in Applied Mechanics and Engineering **273**, 100–118 (2014)
9. Bourdin, B., Francfort, G.A., Marigo, J.J.: Numerical experiments in revisited brittle fracture. Journal of the Mechanics and Physics of Solids **48**(4), 797–826 (2000)
10. Bourdin, B., Marigo, J.J., Maurini, C., Sicsic, P.: Morphogenesis and propagation of complex cracks induced by thermal shocks. Physical Review Letters **112**, 014,301 (2014)
11. Chukwudozie, C.: Application of the variational fracture model to hydraulic fracturing in poroelastic media. Ph.D. thesis, Louisiana State University, Craft & Hawkins Department of Petroleum Engineering (2016)
12. Detournay, E., Cheng, A.H.D.: Fundamentals of poroelasticity pp. 113–171 (1995)
13. Francfort, G.A., Marigo, J.J.: Revisiting brittle fracture as an energy minimization problem. Journal of the Mechanics and Physics of Solids **46**(8), 1319–1342 (1998)
14. Garagash, D.I.: Propagation of a plane-strain hydraulic fracture with a fluid lag: Early-time solution. International Journal of Solids and Structures **43**, 5811–5835 (2006)
15. Geertsma, J., de Klerk, F.: A rapid method of predicting width and extent of hydraulically induced fractures. Journal of Petroleum Technology **21**(12), 1571–1581 (1969)
16. Hattori, G., Trevelyan, J., Augarde, C.E., Coombs, W.M., Aplin, A.C.: Numerical simulation of fracking in shale rocks: current state and future approaches. Archives of Computational Methods in Engineering **24**(2), 281–317 (2017)
17. Henry, H., Levine, H.: Dynamic instabilities of fracture under biaxial strain using a phase field model. Physical Review Letters **93**(10), 105,504 (2004)
18. Karma, A., Kessler, D.A., Levine, H.: Phase-field model of mode iii dynamic fracture. Physical Review Letters **87**(4), 045,501 (2001)
19. Khristianovic, S.A., Zheltov, Y.P.: Formation of vertical fractures by means of highly viscous liquid. In: Fourth World Petroleum Congress Proceedings, pp. 579–586 (1955)
20. Landau, L.D., Lifshitz, E.M.: Statistical Physics. Pergamon Press, Oxford (1980)
21. Lillies, A.T., King, S.R., et al.: Sand fracturing with liquid carbon dioxide. In: SPE Production Technology Symposium. Society of Petroleum Engineers (1982)
22. Manthei, G., Eisenblätter, J., Kamlot, P.: Stress measurements in salt mines using a special hydraulic fracturing borehole tool. PDF). In Natau, Fecker & Pimentel. Geotechnical Measurements and Modelling pp. 355–360 (2003)
23. Middleton, R., Viswanathan, H., Currier, R., Gupta, R.: Co2 as a fracturing fluid: Potential for commercial-scale shale gas production and co2 sequestration. Energy Procedia **63**, 7780–7784 (2014)
24. Miehe, C., Hofacker, M., Welschinger, F.: A phase field model for rate-independent crack propagation: Robust algorithmic implementation based on operator splits. Computer Methods in Applied Mechanics and Engineering **199**(45-48), 2765–2778 (2010)

25. Miehe, C., Welschinger, F., Hofacker, M.: Thermodynamically consistent phase-field models of fracture: Variational principles and multi-field FE implementations. International Journal for Numerical Methods in Engineering **83**, 1273–1311 (2010)
26. Sargado, J.M., Keilegavlen, E., Berre, I., Nordbotten, J.M.: High-accuracy phase-field models for brittle fracture based on a new family of degradation functions. ArXiv e-prints (2017)
27. Span, R., Wagner, W.: A new equation of state for carbon dioxide covering the fluid region from the triple-point temperature to 1100 k at pressures up to 800 mpa. Journal of physical and chemical reference data **25**(6), 1509–1596 (1996)
28. Suehiro, Y., Nakajima, M., Yamada, K., Uematsu, M.: Critical parameters of {xCO 2+(1- x) CHF 3} forx=(1.0000, 0.7496, 0.5013, and 0.2522). The Journal of Chemical Thermodynamics **28**(10), 1153–1164 (1996)